Several Phenomena under High Pressure

By
Tamiyuki EGUCHI** and Shinroku SAITO*

Reprinted from

The Bulletin of The Tokyo Institute of Technology

Number 103, 81 — 98

March 31, 1971

BULLETIN OF THE TOKYO INSTITUTE OF TECHNOLOGY *Number 103*, **1971**
669 541.12.034 66-987

Several Phenomena under High Pressure

By
Tamiyuki EGUCHI** and Shinroku SAITO*

In this paper, are treated pressure calibration and distribution in a sample assembly, variations of ionic radii in alkali alides under high pressure and effect of pressure on the eutectic temperature of the bismuth-cadmium binary system.

1. Pressure Calibration and Pressure Distribution

The high pressure apparatus used for the investigations was the modified piston-cylinder devices which was developped by Kennedy[1]. The schematic representation of this apparatus is shown in Fig. 1. The only difference between our apparatus and that of Kennedy was the absence of the lever arm for rotation of a piston which Kennedy used to relieve the friction in a sample cell. The pressure calibration was performed by observing the phase transitions of bismuth and changes in electric resistance of manganin wire. The sample assemblies for bismuth (prepared by Mitsubishi Kinzoku Kogyo Co., Ltd.) and manganin wire (prepared by Toshiba Denki Co., Ltd.) are represented in Fig.

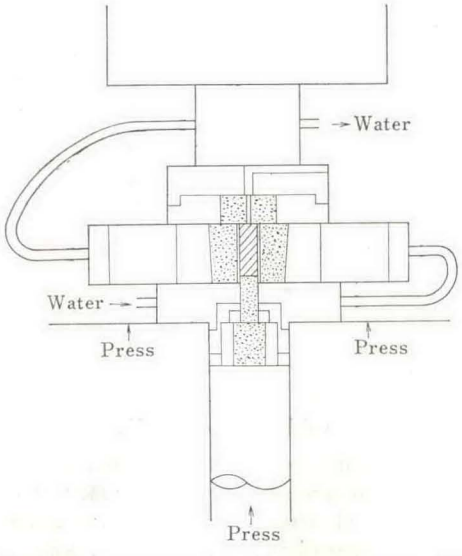

Fig. 1. The schematic representation of our apparatus. Water is flowed in high temperature experiment. Press loading was measured by the Heise Gauge (Heise Bourdon Tube Comp. Inc.)

* Professor, Dr. Sci. in Eng.
** Graduate Student

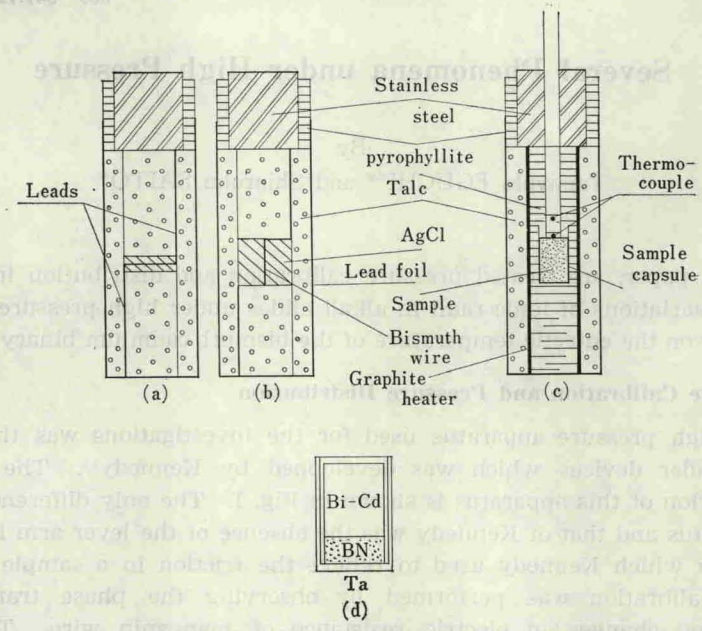

Fig. 2. Sample assemblies; we used (a) for the pressure calibration, (a), (b) for the measurement of pressure distributions and (c) for high temperature experiments. (d) shows the typical sample capsule for high temperature experiments.

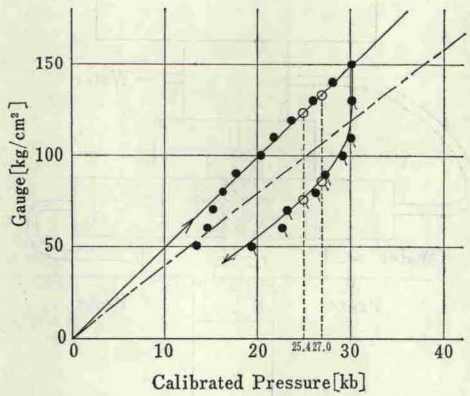

Fig. 3. The pressure calibration curve for our apparatus at room temperature; ○, ○, the transition pressures of bismuth; ●, ●, the observed values obtained from the electrical resistance of manganin wire. The assembly for this experiment is shown in Fig. 2-(a).

2(a) and Fig. 2(b). Bismuths used for the calibration had the purity of 99.999% and the impurities were Au, Ag, Cu, Pb, Fe, Sb and As. As the fixed points [1], the bismuth I-II transition at 25.4kb and the bismuth II-III transition at

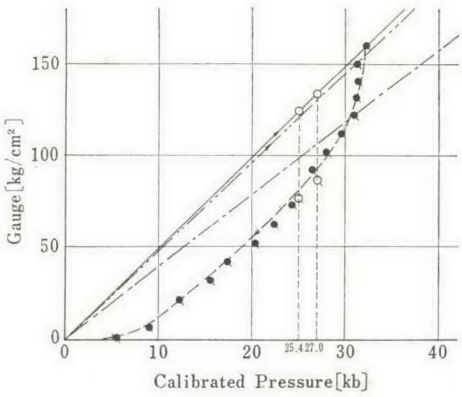

Fig. 4. The pressure calibration curve at high temperature (200—300°C), which was determined by the indirect method as described in "Discussion".

27.0kb were choosed. These transitions were noted on X-Y recorder as discontinuities of the electrical resistance. Manganin wire was used to note the linearity of calibration curve. The all experiments described above were made at room temperature and the results are shown in Fig. 3.

To calibrate applied pressure at high temperature (200-300°C), the melting curve of bismuth was utilized, which was obtained by the experiment of Kodama [2]. At a given melting temperature, the melting of bismuth in a sample cell must occur at the same internal pressure in both compression run and decompression run. Therefore, if we increase the internal pressure along the calibration curve at room temperature noting melting points, and then, decrease pressure noting melting points, the calibrated decompression curve can be obtained. But, of course, this calibration curve includes the decreases of frictions in compression run and decompression run. The pressure calibration at high temperature may be performed by dividing these decreases into the part of compression run and that of decompression run. Further details will be explained in "Discussion". The calibration curve at high temperature obtained as described above is shown in Fig. 4, and the assembly for this experiment is shown in Fig. 2(c). One can see from Fig. 4, that the calibration curve at room temperature can be applied to high temperature (200-300°C) experiment.

Fig.'s 5 and 6 show the pressure distributions in the sample assemblies represented in Fig.'s 2(a) and 2(b). The positions of bismuths in the sample assemblies are plotted versus applied pressures, at which the phase transitions of bismuth occurred.

Fig. 2(c) shows a typical sample assembly to supply power. Temperature was measured by the thermocouple being in contact with the top of the sample capsule, and phase transitions were observed by the D.T.A. technique, another thermocouple was set at about 3mm high position from the top of the capsule. The thermocouples were made of chromel and alumel. Effect of pressure on the thermoelectric force was neglected.

We can see from Fig. 3, that the calibration curve in compression run is

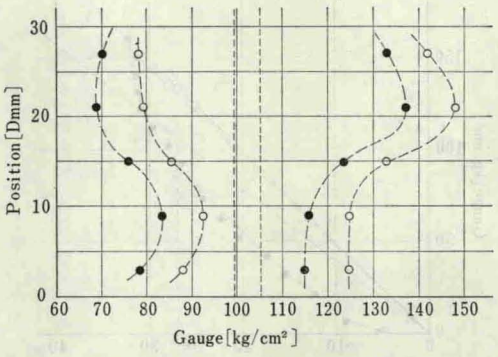

Fig. 5. The pressure distribution in vertical direction in the assembly of Fig. 2-(a). D's show the positions of bismuths measured from the bottom of the assembly.

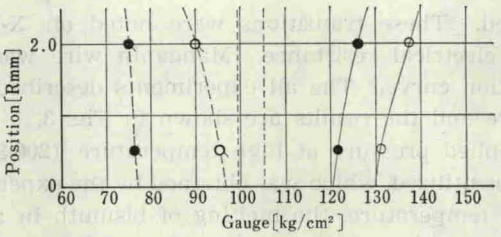

Fig. 6. The pressure distribution in radial direction in the assembly of Fig. 2-(b). R's show the positions of bismuths measured from the center of the assembly.

almost linear. But the linearity could not be verified at low pressure, because the values of electric resistance of manganin wire were scattered. We can see also from Fig. 3, that internal pressure remains high in the first of decompression run. The high value may be lowered in long time, but it may be too long for actual experiment.

The pressure calibration at room temperature can not be applied generally in high temperature experiment, because of changes in internal frictions of pressure transmitting materials and in frictions between the pressure transmitting materials and the face of the cylinder. Decker[3] proposed the equation of state of NaCl and its use as a pressure gauge in high pressure and high temperature research. But this precise equation is not useful as a pressure gauge for the apparatus like piston cylinder devices, because of the difficulty of measurement of the accurate volume change of NaCl at high temperature. Therefore, to calibrate pressure induced by piston cylinder devices at high temperature, an indirect method was made. Assuming that the effects of heat on the frictions are equal in both compression run and decompression run, the pressure calibration at high temperature is performed by noting a certain phase transition such as melting of a proper substance with weak dependence on pressure. In our

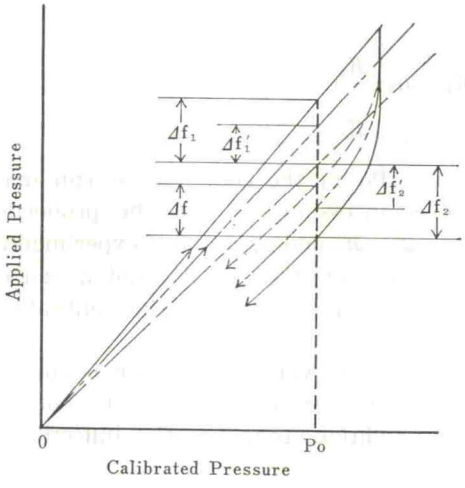

Fig. 7. Calibrated pressure

experiment, the melting curve of bismuth was used. We shall explain the method using Fig. 7.

There are curves of four types in this figure, — shows the calibration curve at room temperature, — shows the ideal curve with no frictions, — shows the calibration curve at high temperature which includes the effects of heat on frictions in compression run and — shows the calibration curve at high temperature which we want. Δf_1, Δf_2, $\Delta f_1'$,$\Delta f'_2$ and Δf are the distances as represented in Fig. 7. Po is a certain fixed point. We used the transition pressures of bismuth as Po's (Note the linearity of curves in this region). The third curve can be obtained as follows. At a given melting temperature, the melting of bismuth in the sample cell must occur at the same internal pressure in both compression run and decompression run. Therefore, if we increase the internal pressure along the calibration curve at room temperature noting melting points, and then, decrease pressure noting mlting points, the calibrated decompression curve is obtained, and then, Δf is obtained. But this curve includes the decreases of the frictions in the two runs. The fourth curve is obtained by dividing these decreases into the part of the compression run and that of the decompression run. The assumption that the effects of heat on the frictions are equal in both compression run and decompression run means

$$\Delta f_1' = (1-\alpha)\,\Delta f_1 \tag{1}$$

and

$$\Delta f_2' = (1-\alpha)\,\Delta f_2. \tag{2}$$

The sum of the decreases of Δf_1 and Δf_2 must be equal to the decrease of frictions included in the decompression curve of the third curve, that is,

$$\Delta f = (\Delta f_1 - \Delta f_1') + (\Delta f_2 - \Delta f_2'). \tag{3}$$

Substituting eq.'s (1) and (2) into eq. (3), we have

$$\alpha = \frac{\Delta f}{\Delta f_1 + \Delta f_2}$$

and

$$\Delta f_1' = \left(1 - \frac{\Delta f}{\Delta f_1 + \Delta f_2}\right) \Delta f_1 \qquad (4)$$

$$\Delta f_2' = \left(1 - \frac{\Delta f}{\Delta f_1 + \Delta f_2}\right) \Delta f_2.$$

The frictions at pressure Po in the compression run may be proportional to Δf_1, and that in the decompression run may be proportional to Δf_2, at room temperature. Moreover Δf_1, Δf_2 and Δf are the experimental values. Therefore, we can caluculate the values of $\Delta f'_1$ and $\Delta f'_2$, and w can obtain the calibration curve at high temperature. Fig. 4 shows the calibration curve obtained by this method.

The pressure distribution in vertical direction is complicated and variations have maximum at the center of the assembly in both compression run and decompression run. In addition, they are the inflection points (See Fig.'s 5 and 6).

References

1) G. C. Kennedy and P. N. LaMori, "Progress in very High Pressure Research", p.304, Willy, New York, (1961).
2) One of the fellows in our laboratory.
3) D. L. Decker, J. Appl. Phys., 36, 157 (1965).

2. Variations of Ionic Radii in Alkali Halides Under High Pressure

Ions in NaCl Structure

At atmospheric pressure, to a fair approximation, ionic radii are additive quantities. In this chapter, it will be examined whether this approximation is also fair at high pressure or not.

The following modified Born-Mayer[1] equation for the lattice energy of an ionic crystal is used in caluculating the P-K relation. K is defined by k=V/Vo, V is the volume of an ionic crystal under pressure P and Vo is the volume of the crystal under zero pressure. The reason why we don't start with experimental values of variations of volumes of ionic crystals under high pressure but theoretical values, will be understood later. The lattice energy E_L is given by

$$E_L = -\alpha \frac{e^2}{a} + Mb \exp\left(-\frac{a}{\rho}\right) \qquad (1)$$

where, α, e, a, and M, are the Madelung constant, the electric charge of an electron, the nearest neighbor distance and the coordination number. b, p are the experimental parameters. Using the equilibrium condition $dE_L/da=0$ and notation a_0 as th nearest neighbor distance at zero pressure and absolute zero, we have

$$E_L = -\alpha \frac{e^2}{a} + \frac{\alpha e^2 \rho}{a^2} \exp\left(-\frac{a_0 - a}{\rho}\right). \qquad (2)$$

If we consider the thermal term at finite temperature, the internal energy is written in the form

$$E = E_L + E_K,$$

where E_K is the kinetic energy and E_L is of eq. (1). And the equation of state is

$$P - T \cdot \frac{\beta}{K} - \frac{dE_L}{dV} - \left(\frac{\partial E_K}{\partial V}\right)_T \tag{3}$$

where β, K are the coefficient of thermal expantion and the isothermal compressibility of the ionic crystal. As far as we are concerned with the problem near room temperature, we can neglect the entropy term and the kinetic energy term in eq. (3). We can say this by comparing our results with other authors'[1) 2) 3)]. Hence E_L in eq. (2) may be considered as the internal energy of the ionic crystal at room temperature, and eq. (3) becomes

$$P = \frac{\alpha e^2 a}{3V}\left\{\frac{1}{a_0^2}\exp\left(\frac{a_0 - a}{\rho}\right) - \frac{1}{a^2}\right\}. \tag{4}$$

The relation between volume and the nearest neighbor distance is of the form

$$V = c\,Na^3, \tag{5}$$

where c is a constant value determined from the crystal structure and N is the number of positive or negative ions in the crystal. For the NaCl structure c is 2, and eq. (4) becomes

$$P = \frac{\alpha}{6} \cdot \frac{e^2}{K^{4/3} a_0^4}\left[K^{2/3}\exp\left\{\frac{a_0}{\rho}(1 - K^{1/3})\right\} - 1\right] \tag{6}$$

where K is defined as $K = (a/a_0)^3$.

The unknown parameter p is determined from the compressibility Ko at room temperature and atmospheric pressure which has the relation between the lattice energy as

$$\frac{1}{K_0 V_0} = \left(\frac{d^2 E_L}{dV^2}\right)_{V_0}, \tag{7}$$

substitution of eq. (2) into eq. (7) yields

$$\frac{a_0}{\rho} = \frac{18 a_0^4}{K_0 \alpha e^2} + 2. \tag{8}$$

In Table 1. the compressibilities K_0's, the nearest neighbor distances a_0's[4)], the calculated a_0/p's and p's are given. The P-K relations are shown in Fig. 1. Here we compare our results with the experimental values of Bridgman[5)] (we extended the calculations to the slable regions of the CsCl structure for some alkali halides). NaI shows considerable discrepancy between the calculated values and the observed values, this may be due to the small effective number of two of the observed compressibility. Hence we shall exclude LiI, NaI, KF and RbCl (These have the effective number of two, others have three) in calculating the ionic radii at high pressure (we shall calculate the ionic radii last of all). Fig. 2 shows P-a relations which were calculated to examine additive character of ionic radii at high pressure.

At atmospheric pressure, to a fair approximation, ionic radii are additive quantities. We shall examine whether this approximation is also fair at high pressure or not. The examination is made as follows. We denote AX as a certain alkali halide. A is an alkali metal ion and X is a halide ion. The additive character of ionic radii is shown by the equations

$$AX - A'X = AX' - A'X' = \cdots\cdots$$

or

$$AX - AX' = A'X - A'X' - \cdots\cdots$$

Table 1.

Compound	$K_0 \times 10^{12}\left(\frac{cm^2}{dyn}\right)$ T=273°C, P=0	a (A) T=273°C, P=0	a_0/ρ	ρ (A)
LiF	1.53	2.008	6.747	0.299
LiCl	3.48	2.563	7.540	0.350
LiBr	4.28	2.756	8.022	0.344
LiI	7.2	3.040	7.299	0.421
NaF		2.312		
NaCl	4.16	2.812	8.715	0.323
NaBr	5.09	2.978	8.903	0.335
NaI	7.1	3.225	8.807	0.367
KF	3.3	2.669	8.870	0.307
KCl	5.64	3.137	9.670	0.324
KBr	6.66	3.290	9.859	0.334
KI	8.54	3.522	10.05	0.350
RbF		2.815		
RbCl	7.4	3.262	8.835	0.369
RbBr	7.95	3.437	9.842	0.350
RbI	9.58	3.664	10.41	0.352

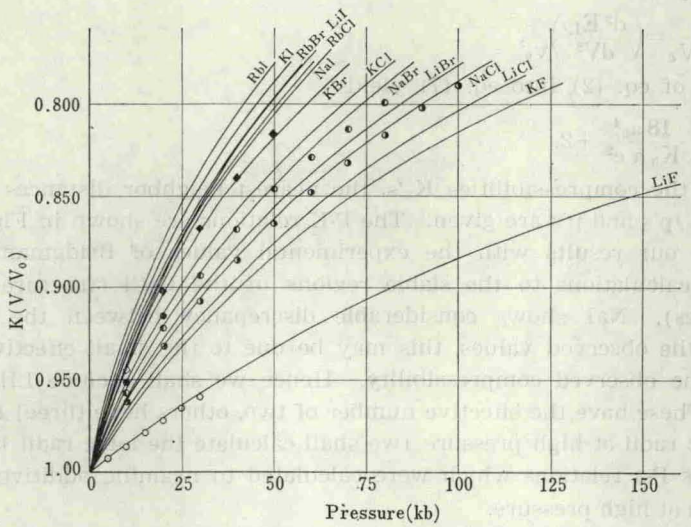

Fig. 1. The volume decreases of alkali halides in the NaCl structure as a function of pressure. Solid curves, the calculated results (extended to pressure range in which the CsCl structure is more stable for some alkali halides). The observed values (5), ○ LiF, ● KCl, ◑ NaCl, ◐ NaBr, ◇ KBr, ◆ NaI.

The equalities are fairly satisfied at atmospheric pressure. So, if we examine these differences at high pressure, we can see whether the additive character

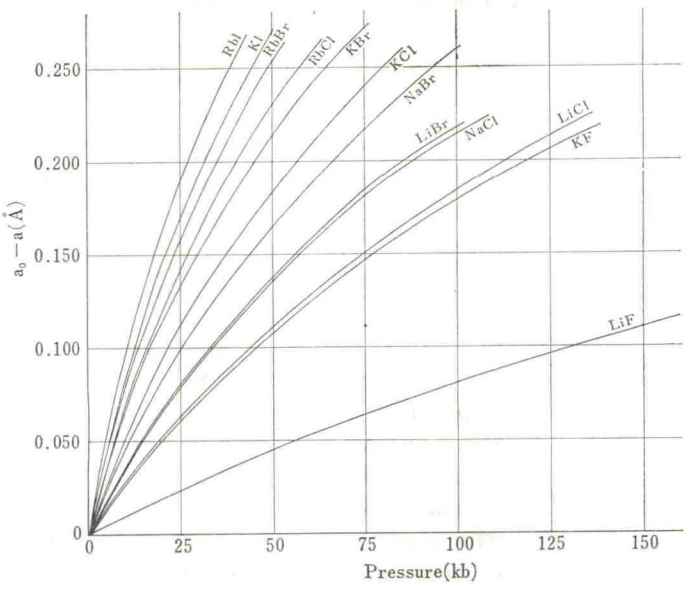

Fig. 2. The shortest interionic distances of alkali halides in the NaCl structure as a function of pressure.

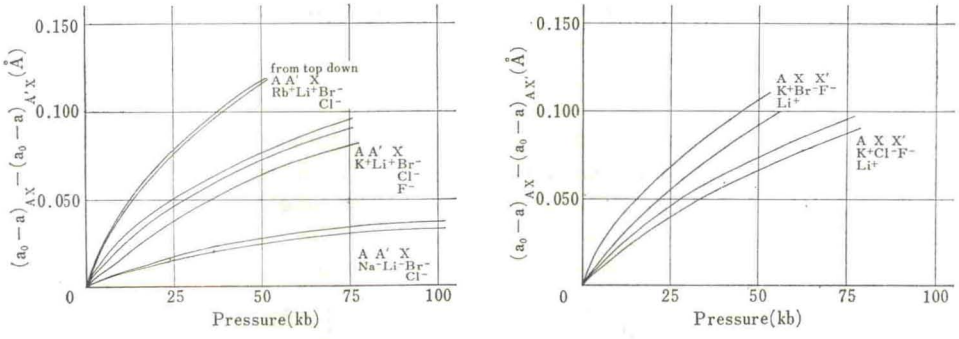

Fig. 3 and Fig. 4. The examinations of the additive character of the ionic radii in the NaCl structure.

becomes better or not increasing pressure. In Fig.'s 3 and 4 the calculated results are given. We can say that the approximation is also fair at high pressure, but not so fair as at atmospheric pressure. The ions in the CsCl structure will be treated in the next part B.

Ions in CsCl structure

The alkali halides except CsCl, CsBr and CsI have the NaCl structure at atmospheric pressure. But, increasing pressure, some alkali halides transform to the CsCl structure[5]. The theoretical treatments of the transitions of these

Table 2. Calculated values of a'_0's and a'_0/ρ's

Compound	a'_0(A) T=273°C, P=0	a'_0/ρ
KCl	3.250	10.02
KBr	3.460	10.21
KI	3.642	10.39
RbCl	3.394	9.198
RbBr	3.558	10.19
RbI	3.785	10.75

alkali halides are as follows[1]. We assume that the experimental parameters b and p in eq. (1) are independent of pressure and structures. With this assumption a'_0 for the CsCl structure corresponding to a_0 for the NaCl structure can be calculated. Substituting a'_0 instead of a_0 into eq. (2), we can calculate the lattice energies of those alkali halides in the CsCl structure and then, the Gibbs' free energies. The stability of a structure is determined by the magnitude of the Gibbs' free energy for each structure. The Gibbs' free energy of each alkali halides except CsCl, CsBr and CsI has a smaller value in the NaCl structure than that in the CsCl structure below the transition pressure. Therefore a'_0's of those alkali halides are the imaginary nearest neighbor distances in the CsCl structure. However, these a'_0's are useful to examine the additive character of ionic radii in the CsCl structure. The imaginary nearest neighbor distance a is calculated by the equation

$$\frac{1}{a'^2_0}\exp\left(\frac{a'_0}{\rho}\right)=\frac{8\alpha}{6\alpha'}\cdot\frac{1}{a_0^2}\exp\left(\frac{a_0}{\rho}\right) \tag{9}$$

where α' is the Madelung constant for the CsCl structure and a_0 is the actual nearest neighbor distance in the NaCl structure at room temperature and atmospheric pressure. In Table 2, the imaginary nearest neighbor distances a'_0's and a'_0/ρ's of some alkali halides are given.

Using a'_0 and c $(=2/\sqrt{3})^3$) in eq. (5), eq. (6) becomes

$$P=\frac{\alpha'}{4.611}\cdot\frac{e^2}{K'^{4/3}a'^4_0}\left[K'^{2/3}\exp\left\{\frac{a'_0}{\rho}(1-K'^{1/3})\right\}-1\right] \tag{10}$$

where K' is defined as $K'=(a'/a_0')^3$ and a' is the nearest neighbor distance in the CsCl structure at pressure P. The calculated results of P-K' relations are shown in Fig. 5. Here we extended the calculations to the pressure regions in which the NaCl structure is more stable for same alkali halides. Fig. 6 shows P-a' relations which are calculated to examine additive character of ionic radii at high pressure. We compare our results with the observed values by Bridgman[5] in Fig. 5. The imaginary nearest neighbor distances were obtained by the extrapolations in these cases. Here the solid curves (except the curves for CsCl, CsBr and CsI which were observed by Bridgman[5] show the calculated results. In this case, the discrepances between the calculated results and the observed values are rather large. However we must be careful about the observed values and the extrapolated values of $V_0'[=(2/\sqrt{3})^3a_0^3]$. The later values are determined predominantly from the observed values in the small

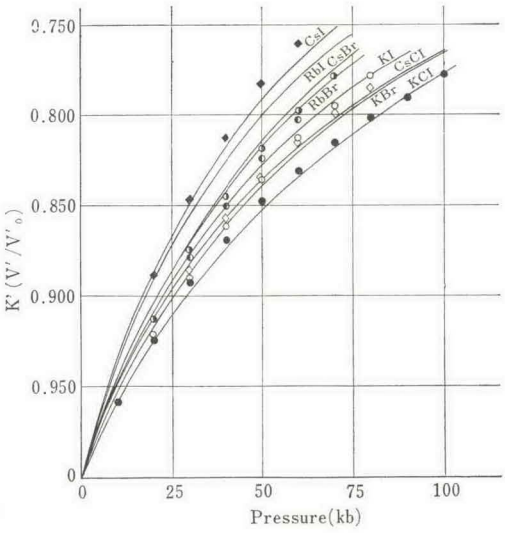

Fig. 5. The volume decreases of alkali halides in the CsCl structure as a function of pressure. Solid curves (except the curves for CsCl, CsBr and CsI, which were observed by Bridgman), the calculated results (extended to the pressure range in which the NaCl structure is more stable for some alkali halides). The observed values (5), ● KCl, ○ RbCl, ◇ KBr, ◐ RbBr, ◑ KI, ◆ RbI.

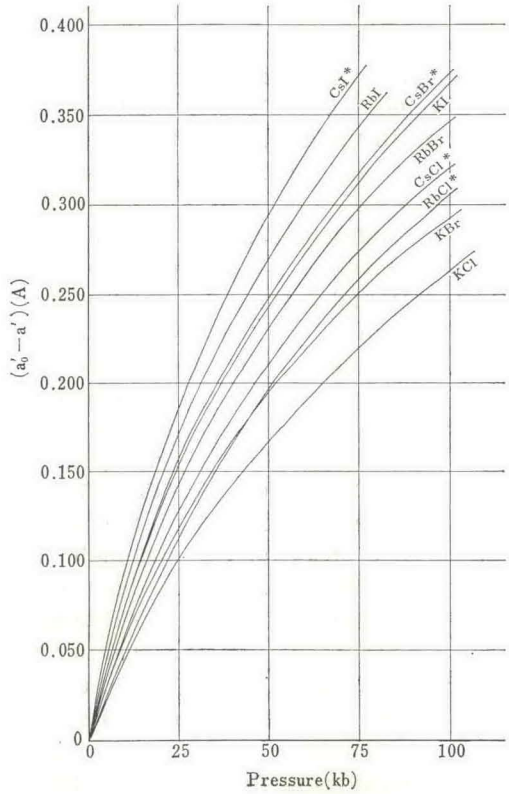

Fig. 6. The shortest interionic distances of the alkali halides in the CsCl structure as a function of pressure.

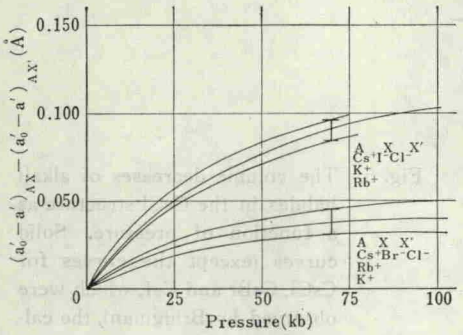

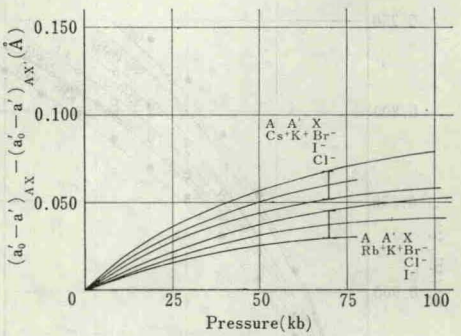

Fig. 7 and Fig. 8. The examination of the additive character of the ionic radii in the CsCl structure.

pressure ranges after the transitions and the slopes at the transition pressures. If a transition is not terminated completely at the transition pressure, the slope at the pressure must be larger than that at the pressure at which the transition is terminated completely. This yields the larger value of V'_0 and the smaller value of K'. We see in Fig. 5 that, for example, RbI is observed more compressible than CsI. But this may not be true and must be due to the fact that the transition of RbI is not terminated completely at the transition pressure. Therefore we shall use the calculated values for KCl, KBr, KI, RbBr, RbI and the observed values for CsCl, CsBr, CsI, in examining the additive character of the ionic radii in the CsCl structure.

The additive character of ionic radii at high pressure are examined by the similar manner in the last Part A., and this is made in Fig.'s 7 and 8. We may say that the ionic radii are additive quantities at high pressure, but the additive character becomes slightly worse as increasing pressure.

We can see in Fig.'s 1 and 5 that the eq. (1) gives good results. The approximation that the ionic radii are additive quantities may be also fair at high pressure, but not so fair as at atmospheric pressure. An ion surrounded by small ions may be more compressible than the ion surrounded by large ions. This character grows evident with increasing pressure for the ions in the CsCl structure (See Fig.'s 7 and 8), but this character is nearly independent of pressure for the ions in the NaCl structure (See Fig.'s 3 and 4). These tendencies may be due to the repulsive interactions between the second nearest neighbors.

Even though the additive character of ionic radii has these tendencies, it may be useful to determine the ionic radii at high pressure. The repulsive term in the expression (1) of the lattice energy was determined rather ambiguously, because this form was estimated from the quantum mechanical expression of the energy of the hydrogen like molecule[6) 7)]. But, in fact, the interaction between the outermost closed shells of an ion and its nearest neighbors predominantly yields the repulsive energy, because of the Pauli's principle[8)]. Therefore, if we use the wave functions of the outermost electrons expressed by the effective changes of the nuclei screened by the inner electrons, the repulsive term may be expressed by the linear combination of the three different terms

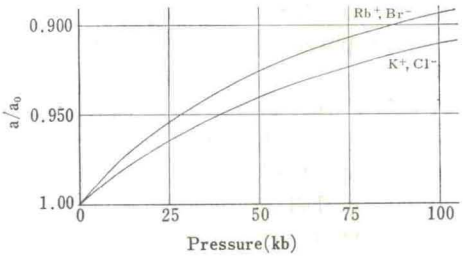

Fig. 9 a. The ionic radii in the NaCl structure as a function of pressure.

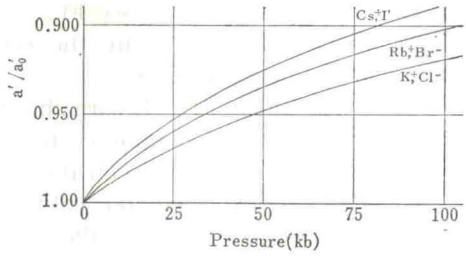

Fig. 9 b. The ionic radii in the CsCl structure as a function of pressure.

which include the factors of exp $(-r/p_A)$. exp $(-r/p_X)$ and $(-r/p_{AX})$ respectively. Here p is the function of the effective charge of the nucleus for the outermost electrons of the alkali metal ion A and its principal quantum number. Similarly p_X depends on the halide ion X and P_{AX} depends on the two ions. However the precise form of the repulsive term including these factors may be very complicated. Whereas, the simple expression (1) gives good results. Therefore we may consider the repulsive term in the expression (1) as the average of those complicated expression. Moreover p in the eq. (1) is a constant value, so, we may consider that the effective charges of the nuclei for the outermost electrons are nearly independent of pressure. And we can calculate the ionic radii at high pressure following Pauling[9]. Fig.'s 9a and 9b show the results, in which the ionic radii in the NaCl structure and the ionic radii in the CsCl structure are given as a function of pressure.

References

1) M. Tosi and T. Arai, "Advance in High Pressure Research" vol. 1, edited by R. S. Bradley, p.265, Academic Press, London (1966).
2) M. P. Tosi and F. G. Fumi, J.P.C.S. **23**, 359, (1961).
3) P. L. Decker, J.A.P., **36**, 157, (1965).
4) "International Critical Table", McGraw Hill, New York, (1933).
5) P. W. Bridgman, "Collected Experimental Papers", Harvard University Press, Cambridge, Massachusetts, (1964).
6) L. Pauling, ZS. f. Phys., **67**, 377, (1928).
7) M. Born and J. E. Mayer, ZS. f. Phys, **75**, 1, (1932).
8) J. C. Slater, "Quantum Theory of Matter", chapter 9, McGraw Hill, New York, (1951).
9) L. Pauling, Proc. Roy, Soc., London, A. 114, 181, (1927), J. Am. Chem. Soc., **49**, 765, (1927).

3. Effect of Pressure on the Eutectic Temperature of Bismuth-Cadmium System up to 30kb

The sample assembly for this investigation is shown in Fig. 2(c) in chapter 1. The pressure calibration at room temperature was used in this high temperature (up to 500°C) experiment, because the frictions may be almost same as

that at room temperature (See Fig. 4 in chapter 1). The same bismuth as that in chapter 1 was used again, the cadmium (prepared by Junsei Kagaku Co., Ltd.) had the purity of 99.9%.

The experimental results are shown in Fig.'s 1, 2(a) and 2(b). Fig. 1, shows the phase diagram of cadmium, our result agrees with that of Kennedy[1] quite well. The effect of pressure on the eutectic temperature is shown in Fig.'s 2(a) and 2(b). The experimental values obtained by D.T.A. technique were not sufficiently correct, especially the signals to determine the solidification curves

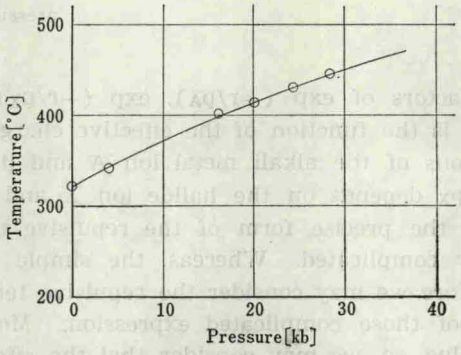

Fig. 1. The phase diagram of cadmium. The solid curve was the observed one by Kennedy[1] and circles show our results.

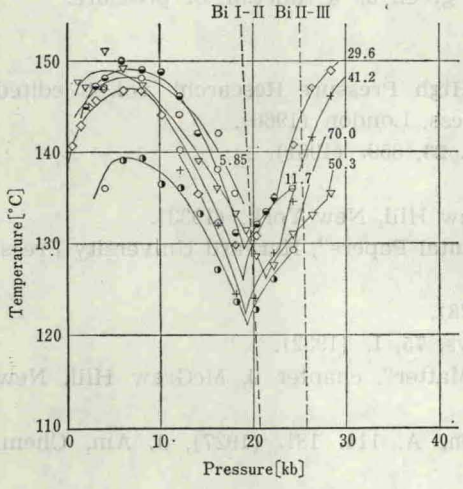

Fig. 2-(a). The effect of pressure on the eutectic temperature of Bi-Cd system. Numerical values show the weight percentages of cadmium. The results in 6 runs of 11 runs are given to avoid unimportant complexity.

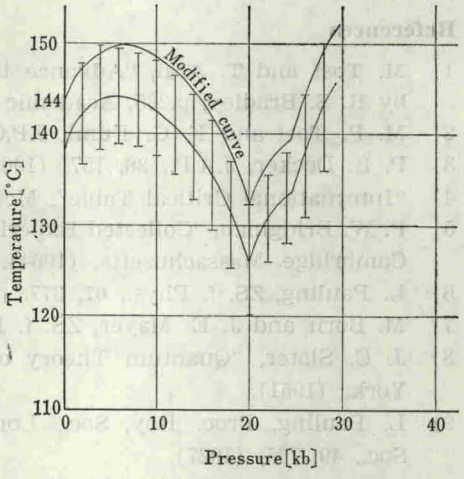

Fig. 2-(b). The lower curve shows the average of the direct experimental results (Fig. 2-(a)) and the upper curve shows its modification which was obtained by its parallel displacement.

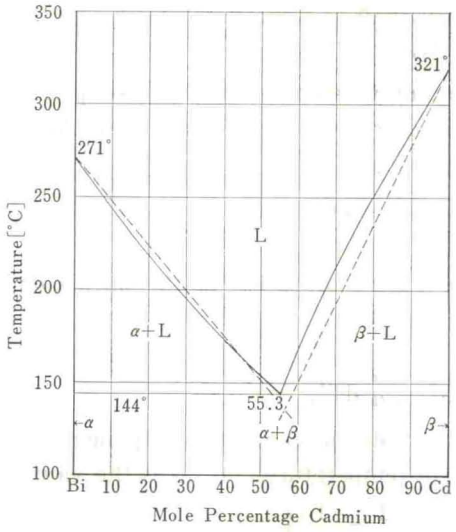

Fig. 3. The phase diagram for Bi-Cd system at atmospheric pressure. The solid curve shows the observed result and[2] the dashed curve shows the calculated result.

were ambiguous or not appeared. But, nevertheless, the curves obtained in 11 runs had the same figure, that is, the figure shows the effect of pressure on the eutectic point.

In fact, we could not obtain correct solidification curves at high pressure. But ambiguous signals on a solidification curves were appeared sometimes, and we can say that the composition at the eutectic point may be nearly independent of pressure.

Now, we shall consider thermodynamically the Bi-Cd system. The solid curve in Fig. 3 shows the phase diagram for Bi-Cd system at atmospheric pressure[2]. In two components (say α and β) system such as bismuth and cadmium the chemical potentials for component α and component β in liquid phase are generally given by

$$\mu_\alpha^1 = \mu_\alpha^{\circ 1} + RT \ln x\alpha\, \gamma\alpha, \tag{1}$$

and

$$\mu_\beta^1 = \mu_\beta^{\circ 1} + RT \ln x\beta\, \gamma\beta, \tag{2}$$

where a, 1, γ's, and x's mean a pure component, liquid phase, activity coefficients and mole fractions. On the solidification curves, the following relations must be satisfied,

$$\mu_\alpha^{\circ S} = \mu_\alpha^1 = \mu_\alpha^{\circ 1} + RT \ln x\alpha\, \gamma\alpha \tag{3}$$

and

$$\mu_\beta^{\circ S} = \mu_\beta^1 = \mu_\beta^{\circ 1} + RT \ln x\beta\, \gamma\beta, \tag{4}$$

where s means solid phase. Eq. (3) becomes

$$\ln x\alpha\,\gamma\alpha = -\frac{\mu_\alpha^{\circ 1} - \mu_\alpha^{\circ S}}{RT} = -\frac{\Delta\mu_\alpha^0}{RT}. \tag{5}$$

$\Delta\mu_\alpha^{\circ}$ is the function of only temperature, because pressure is keeped constant at Po. So $\Delta\mu_\alpha^{\circ}$ is derived from the latent heat of fusion of the pure component α by the equation

$$\left[\frac{\partial}{\partial T}\left(\frac{\Delta\mu_\alpha^{\circ}}{T}\right)\right]_{P_0} = -\frac{\Delta h_\alpha^{\circ}}{T^2}, \tag{6}$$

where Δh_α° is the latent heat of fusion of the pure component α. Integrating eq. (6), we have

$$\Delta\mu_\alpha^{\circ} = -T\int_{T_\alpha^{\circ}}^{T} \frac{\Delta h_\alpha^{\circ}}{T'^2}\,dT', \tag{7}$$

where T_α° is the melting point of the pure component α at pressure Po. If Δh_α° is nearly independent of temperature and takes the value at T_α°, eq. (7) becomes

$$\Delta\mu_\alpha^{\circ} = -T\Delta h_\alpha^{\circ}\left(-\frac{1}{T}+\frac{1}{T_\alpha^{\circ}}\right)$$

and eq. (5) becomes

$$\ln x_\alpha\,\gamma_\alpha = \frac{\Delta h_\alpha^{\circ}}{R}\left(-\frac{1}{T}+\frac{1}{T_\alpha^{\circ}}\right), \tag{8}$$

similarly, we have

$$\ln x_\beta\,\gamma_\beta = \frac{\Delta h_\beta^{\circ}}{R}\left(-\frac{1}{T}+\frac{1}{T_\beta^{\circ}}\right). \tag{9}$$

For Bi-Cd system, α, β correspond to bismuth and cadmium. Δh_α°, Δh_β°, T_α° and T_β° are 2.60 kcal/col, 1.53 kcal/mol, 271°C and 321°C[3]. We assume the liquid phase as the ideal solution in the first place. Eq.'s (8) and (9) become

$$\ln(1-x) = 1.30\left(-\frac{1}{T}+\frac{1}{544}\right)\cdot 10^3$$

and

$$\ln x = 0.765\left(-\frac{1}{T}+\frac{1}{594}\right)\cdot 10^3. \tag{11}$$

Eq's (10) and (11) determine the solidification curves and the eutectic point. The calculated results are given by the dashed curves in Fig. 3, which agree well with the experimental result as a whole. Therefore, the liquid phase may be considered as a nearly ideal solution.

Next, we shall consider the effect of pressure on the eutectic point. The differencial of eq. (5) becomes

$$d\ln x_\alpha = -d\left(\frac{\Delta\mu_\alpha^{\circ}}{RT}\right). \tag{12}$$

Here, we make the approximation of $\gamma_\alpha = 1$. This is equivalent to

$$-\Delta S_\alpha^{\circ}\,dT + \Delta V_\alpha^{\circ}\,dp + \frac{RT}{x_\alpha}\,dx_\alpha = 0 \tag{13}$$

where, $\Delta S^{\circ}_{\alpha}$ and $\Delta V^{\circ}_{\alpha}$ are the entropy change and the volume change of component α during melting. Similarly, for component β we have

$$-\Delta S^{\circ}_{\beta}\,dT+\Delta V^{\circ}_{\beta}\,dp+\frac{RT}{x_{\beta}}dx_{\beta}=0. \tag{14}$$

Eq's (13) and (14) must be satistied simultaneously at the eutectic point, so we have

$$\left(\frac{dT}{dp}\right)_{e}=T\frac{x_{\alpha}\Delta V^{\circ}_{\alpha}+x_{\beta}\Delta V^{\circ}_{\beta}}{x_{\alpha}\Delta h^{\circ}_{\alpha}+x_{\beta}\Delta h^{\circ}_{\beta}}. \tag{15}$$

We can calculate the initial slope of the eutectic temperature for Bi-Cd system using eq. (15). Substituting the experimental values[3) 4)], we have

$$\left(\frac{dT}{dp}\right)_{e}=1.02\times10^{-1}\quad[\mathrm{deg\cdot kb^{-1}}].$$

The calculated initial slope has a very small negative value. However, in fact, it has a positive value (see Fig. 2). Therefore, we cannot conclude the character of liquid phase as an ideal solution by considering only the phase diagram at atmospheric pressure.

A general form of eq. (15)[5] is

$$\left(\frac{dT}{dp}\right)_{e}=T\frac{x_{\alpha}\Delta^{l}_{s}V_{\alpha}+x_{\beta}\Delta^{l}_{s}V_{\beta}}{x_{\alpha}\Delta^{l}_{s}h_{\alpha}+x_{\beta}\Delta^{l}_{s}h_{\beta}} \tag{16}$$

where, $\Delta^{l}_{S}h_{\alpha}$ is $h^{l}_{\alpha}-h^{\circ S}_{\alpha}$ and h^{l}_{α} is a partial moler enthalpy of component α in liquid phase, the other notations are defined similarly. We shall explain Fig. 2 using eq. (16). Here, α and β correspond to bismuth and cadmium. At atmospheric pressure $\Delta^{l}_{S}V_{\alpha}$ has a small negative or small positive value, as pressure increases it becomes largely negative, after the transition pressure of bismuth I-II it has a positive or small negative value again, and after the transition pressure of bismuth II-III it has a rather large positive value. This behavior of $\Delta^{l}_{S}V_{\alpha}$ must have some relations with the solid phases of bismuth, but the explanation is difficult even qualitatively.

References

1) G. C. Kennedy and R. C. Newton; "Solid under Pressure", p. 163, McGraw Hill, New York, (1963).
2) "Metal Handbook", edited by T. Lyman, p.1178, The Amer. Society for Metals, Ohio, (1948).
3) "Metals Reference Book", edited by C. J. Smithells, Butter worthe, London, (1967).
4) "International Critical Table", McGraw Hill, New York, (1933).
5) See I. Prigogine et R. Defay, "Thermodynamique Chimique", Desoer, Liége, (1950).